

## ORIGINAL ARTICLE

# Evaluations of Aluminum Tri-Hydroxide and Pristine Montmorillonite in Glass Fiber Reinforced Polymer for Vehicle Components

S. Kaleg<sup>1\*</sup>, A. C. Budiman<sup>1</sup>, A. Hapid<sup>1</sup>, Amin<sup>1</sup>, A. Muharam<sup>1</sup>, Sudirja<sup>1</sup>, D. Ariawan<sup>2</sup>, and K. Diharjo<sup>2</sup><sup>1</sup>Research Center for Electrical Power and Mechatronics, Indonesian Institute of Sciences, Bandung 40135, Indonesia.<sup>2</sup>Department of Mechanical Engineering, Faculty of Engineering, Universitas Sebelas Maret, Surakarta 57126, Indonesia.

**ABSTRACT** – One of the safety requirements for the vehicle components is in terms of the flammability factor. Generally, the polymer material used for vehicle components is Unsaturated Polyester (UP). Unfortunately, this material is highly flammable. The addition of Aluminum Tri-Hydroxide (ATH) to UP is known to improve its flame retardancy, but its material strength is compromised. Moreover, the use of pristine Montmorillonite (MMT) rather than the commonly used organomodified MMT as a mixture to the ATH results in different material characteristics that could potentially minimise such a reduction of material strength. This manuscript discusses the combination of ATH and MMT in Glass Fiber Reinforced Polymer (GFRP) composites, specifically in terms of mechanical properties and flame retardancy. The increase of ATH content to UP decreases the flexural strength of GFRP, ranging from 34.3% to 63.4% lower than the neat GFRP. A slight increase of flexural strength is found in samples with ATH and MMT combinations (CA45M15), indicating that the addition of MMT does not dramatically change the flexural strength of GFRP. However, the addition of filler ATH, MMT, or a combination of both could increase the flame retardancy of GFRP. The addition of ATH leads to a slight increase of the UP initial temperature of decomposition, while the addition of MMT shows almost no notable differences. The flammability test shows that the additions of ATH, MMT or their combinations tend to decrease the rate of linear burning. Therefore, it can be concluded that the ATH and MMT could effectively improve the flame retardancy of GFRP.

**ARTICLE HISTORY**Received: 21<sup>st</sup> June 2021Revised: 30<sup>th</sup> Nov 2021Accepted: 3<sup>rd</sup> Jan 2022**KEYWORDS**

*Aluminum tri-hydroxide;  
Pristine montmorillonite;  
Unsaturated polyester;  
Flame retardancy;  
Mechanical properties*

## INTRODUCTION

Polymers and composites in the automotive industry sector show an increase in the types of materials and components made [1]. Several factors that attract the automotive industry's interest to substitute metal components with polymers are economic value, weight reduction, more flexible shape potential, more functional design, new surface effects, lower maintenance costs, and corrosion resistance [2][3]. The utilisation of plastic allows the design of cars and lightweight vehicles to be more stepping forward by providing style and interior flexibility for designers [4]. Compared to metals such as mild steel, the function of using polymer composites can be adapted to the needs of automotive components. The combination of strength and weight of components can be designed optimally. Examples of composite applications in the automotive field include pistons, brake friction materials, anti-roll bars, and low-velocity impact structures [5]. In electric vehicles, structural battery composites are developed from polymer materials, namely carbon fibre reinforced polymer [6]. However, composite polymers for automotive materials still require some essential factors, such as resistance to temperature, flame retardancy, chemical resistance, wear resistance, impact strength, and resistance to ultraviolet radiation. One of the safety requirements for the vehicle components is in terms of the flammability standard. The commonly used standard for the vehicles components flammability is found in the FMVSS (Federal Motor Vehicle Safety Standard) number 302, which states that the material must not ignite or spread the fire at a rate of burning of more than 4 inches (100 mm) in a minute [7]. Composite materials must be able to withstand fire and produce as little smoke as possible to allow passengers in the vehicle to be evacuated safely [8]. The test results using the FMVSS 302 method on non-flame retardant fabrics show that such materials could produce foam that can cause flames to ignite [9]. Therefore, the fire behaviour of composite polymers for automotive materials is a concern hence the evaluation of their flame retardancy is mandatory [10]. This material must be fire-resistant or burn but with a rate of burning that meets the standards to allow sufficient evacuation time in the event of a fire.

Various thermoset polymer materials can be used for automotive component applications, such as unsaturated polyester [11], epoxy [12], acrylic [13], polyurethane [14], and vinyl ester [15]. Generally, the polymer material used for vehicle components is unsaturated polyester (UP). The UP is relatively cheap, has good mechanical properties, ease of the production process, and is easy to combine with various fibre and fillers, which makes UP in great demand for many engineering applications [16]. Its low material density is also one of the reasons why UP is highly used in the industry and the automotive [17]. However, UP is highly flammable and produces a lot of smoke when it burns [18][19]. Carbon monoxide (CO) is a toxic smoke emission from the decomposition of UP which can cause metabolic acidosis and

respiratory acidosis in humans [20]. The improvement of UP flame retardancy can be made with the addition of Aluminum Tri-Hydroxide (ATH) [21], which is then indicated by a decrease in the amount of smoke generated and the Limited Oxygen Index (LOI) [22]. In the event of a fire hazard, the level of safety for a life increases when the smoke produced is successfully lowered [23]. ATH in the UP is more efficient in increasing ignition time as well as reducing CO emission and Peak Heat Release Rate (PHRR) compared to Calcium Carbonate ( $\text{CaCO}_3$ ) [24]. The addition of ATH to the composite does not affect the decomposition mechanism but slows down the rate of residual formation [25]. Another potential attempt to improve UP flame retardancy is adding a clay-based filler [26], such as Montmorillonite (MMT) [27]. The MMT flame retardancy mechanism is a decrease in PHRR [28] due to the formation of a barrier layer on the surface of the polymer [29]. The addition of MMT increases the flame retardancy of the UP by forming the charcoal when thermal decomposition occurs [30]. The UP application for vehicle components is usually combined with another reinforcement to gain good strength. UP resin and glass fibre (GF) can be integrated to form the so-called Glass Fibre Reinforced Polymer (GFRP), which has better mechanical properties than just UP or GF only [16]. The composite strength can be increased by adding multiple GF layers or GF with a higher modulus [31]. As a reinforcement, GF can be combined with other fibre materials to obtain optimal mechanical properties [32]. Even the same fibre material but different formats may increase the stiffness of a composite [33]. GF arrangement in various material density and fibre format in the UP resin yields maximum tensile stress and bending force significantly higher than the UP without reinforcement.

The addition of ATH to the UP resin improves the GFRP flame retardancy, but it also shows a notable decrease in its mechanical properties [34][35]. After all, the high ATH content causes the viscosity of the matrix to increase so that it disrupts the good manufacturing process [36]. Therefore, to minimise the mechanical properties reduction, the ATH content is lowered, and other flame retardant fillers are added [37][38]. For example, clay and ATH can be used together to produce ethylene vinyl acetate (EVA) composites for the production of cable covers [29]. Another alternative is pristine MMT, which is a non-organomodified MMT that relies on the flame retardancy of heat resistance materials and water vapour. Pristine MMT as natural sources are summarised as a particle and layered structure, barrier property, and water sorption [39]. It is found that the LOI of polymer composites increased up to 25.5% with the addition of pristine MMT [40]. Although it may not have better mechanical properties than the organomodified MMT, pristine MMT eliminates processes for modifying the intercalated layers, leading to a drastically cheaper production cost. The evaluation of the combination of ATH and pristine MMT, especially in terms of flame retardancy and its mechanical properties of GFRP composites for vehicle applications, is still relatively rare in the literature.

In this manuscript, the effect of ATH, pristine MMT, or a combination of both with regards to the flame retardancy and mechanical properties of GFRP is experimentally evaluated. The GFRP composites with the variation of ATH and MMT were made using the hand lay-up production method. The mechanical properties under consideration were flexural strength, surface hardness, and density, which are then associated with the morphology of fractured flexural samples. The flame retardancy of the composites was evaluated using thermogravimetric analysis (TGA) and ASTM D635-03. This study could become the basis for applying composite flame retardant materials with optimal mechanical properties for lightweight components in vehicles.

## EXPERIMENTAL MATERIALS AND METHODS

### Materials

In this study, GFRP composite samples were made from unsaturated polyester and the reinforcement's E-glass fibre. The aluminium tri-hydroxide (ATH) and pristine montmorillonite (MMT) are the fillers used as the flame retardant of the composites. Commercial orthophthalic UP resin 268 BQTN from Singapore Highpolymer Chemical Products (SHCP) was used and it had a specific mass of  $1.22 \text{ g/cm}^3$ . The mechanical properties of neat cured UP resin are 59 MPa in tensile strength, 88 MPa in flexural strength, and 156 MPa in compressive strength [16]. General-purpose E-glass fibres of chopped strand mat (EMC200) and woven roving mat (WR200) were used for the reinforcement. Both GF were supplied by Fantatex, and they had a specific mass of  $200 \text{ g/m}^2$ . Such E-glass fibre has a tensile strength of 3100 – 3800 MPa at  $23 \text{ }^\circ\text{C}$  [41]. The ATH BW153 was supplied by Nippon Light Metal Company, Ltd. The ATH had a specific mass of  $2.42 \text{ g/cm}^3$ , Mohs hardness of 3, a refractive index of 1.57, ignition loss of 34.6%, decomposition temperature at approximately  $200^\circ\text{C}$ , water vapour generation  $0.9 \text{ L/g}$ , and endothermic value of  $2.0 \times 10^3 \text{ J/g}$ . Pristine montmorillonite (MMT) was purchased from Cipta Kimia and had a specific mass of  $2.35 \text{ g/cm}^3$ . The UP resin initiator MEPOXE methyl ethyl ketone peroxide (MEKP) was supplied by Kawaguchi Kimia Indonesia.

### Composites Preparation

The ATH and MMT were heated in an air-circulated oven at  $125^\circ\text{C}$  for 30 min and then stored at room temperature. ATH and MMT were mixed with UP using a high-speed mechanical stirrer at 3,000 rpm for 5 min [24]. The mixture of UP and the filler was stored for 5 min to eliminate the bubble. The 1% UP weight of MEKP (1wt%) was added to the mixture, and then was stirred evenly. Furthermore, the mixture was poured into a mould followed by the GF with the configuration shown in Figure 1. The hand lay-up method was used to disperse the GF mixture. The composites were stored cured at room temperature in the moulding for 24 h [22][42][43][44]. Finally, the composites were removed from the mould and then it was post-cured in oven-dried at  $100^\circ\text{C}$  for one hour [31][45]. The name and composition of the composites samples were tabulated in Table 1.

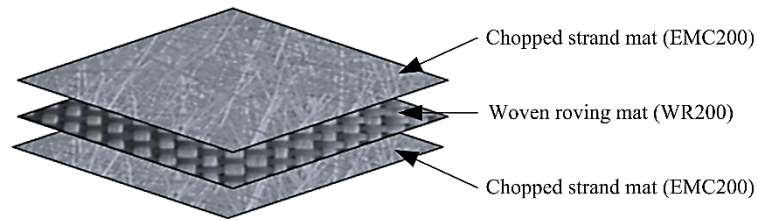


**Figure 1.** GF configuration in the GFRP samples.

**Table 1.** Composition of the samples.

Sample name <sup>1</sup>	GF <sup>2</sup> (layer)	Composition (g)		
		UP	ATH	MMT
C	3	250	-	-
CA10	3	250	25	-
CA20	3	250	50	-
CA30	3	250	75	-
CA40	3	250	100	-
CA50	3	250	125	-
CA60	3	250	150	-
CA45M15	3	250	112.5	37.5
CA30M30	3	250	75	75
CA15M45	3	250	37.5	112.5
CM60	3	250	-	150

<sup>1</sup>) C is GF and UP, A is ATH and M is MMT

<sup>2</sup>) GF configuration follows the configuration illustrated in Figure 1

## Material Characterisations

The mechanical properties of the samples under consideration were flexural strength, surface hardness, composites density, and the morphology of flexural fractured samples using scanning electron microscope (SEM). The flexural strength and flexural modulus following ASTM D6272-00 were obtained from a JTM-UTS510 universal testing machine. The testing configuration was four-point bending with a support span-to-depth ratio of 16.25 and a loading rate of 10 mm/min. The shape of the samples is rectangular with the dimension of length 127 mm, width 12.7 mm, and thick 3.2 mm. The number of four-point bending samples is 5. The Rockwell hardness test following ASTM D785-98 was used to obtain the surface hardness. The hardness test was performed using a Matsuzawa Seiki tester. The surface hardness was measured in Rockwell hardness scale L with 6.35 mm of indenter diameter. The test was performed with a minor load of 10 kg and a major load of 60 kg. The number of surface hardness samples is 5. The composites density measurement was in accordance with ASTM D792-98 and it was compared with the theoretically composites density in accordance with ASTM D2734-94. The percentage of void content was calculated based on both measurement comparisons. The percentage of the voids in the samples can be calculated according to Eq. (1).

$$Void (\%) = 100 \cdot (\rho_T - \rho_M) / \rho_T (\%) \quad (1)$$

where  $\rho_T$  and  $\rho_M$  is the theoretical and the measured sample density in  $g/cm^3$ , respectively. The morphology of flexural fractured samples was observed in a JEOL JSM IT-300 SEM with an accelerating voltage of 20 kV. The samples had cross-sections sputtered with a gold layer before SEM observation.

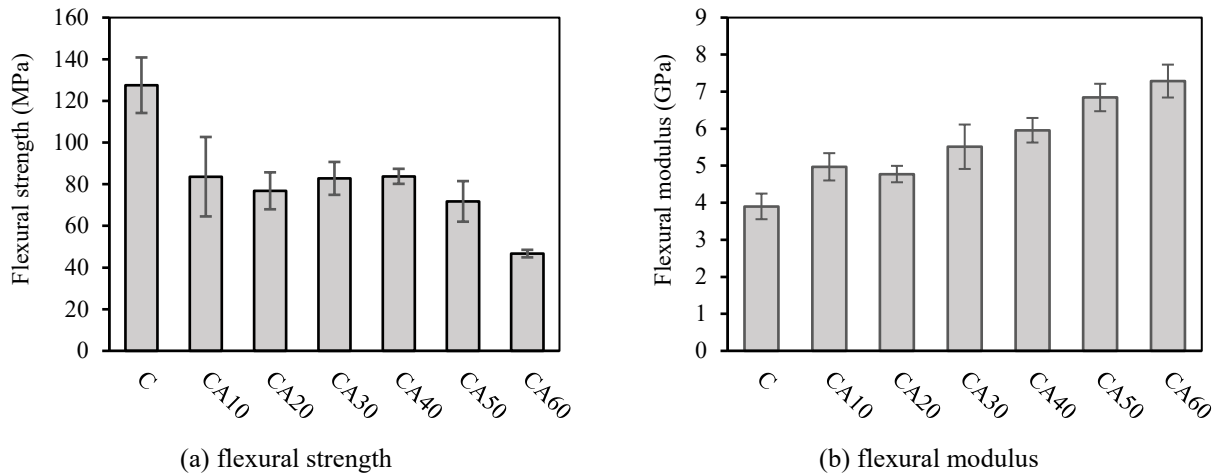
The flame retardancy of the composites was evaluated by means of thermogravimetric analysis using a PerkinElmer STA 6000, at a heating rate of 20 °C/min and a temperature range of 50 °C to 600°C in a nitrogen ( $N_2$ ) atmosphere of 20 mL/min. The flammability test was performed in accordance with ASTM D635-03, which resulted in the rate of linear burning (ROB). The dimensions of the rectangular samples were  $125 \times 13 \times 3.2 \text{ mm}^3$  and the average value was taken from 10 tested samples.

## RESULTS AND DISCUSSION

### Mechanical properties of GFRP filled with ATH and MMT

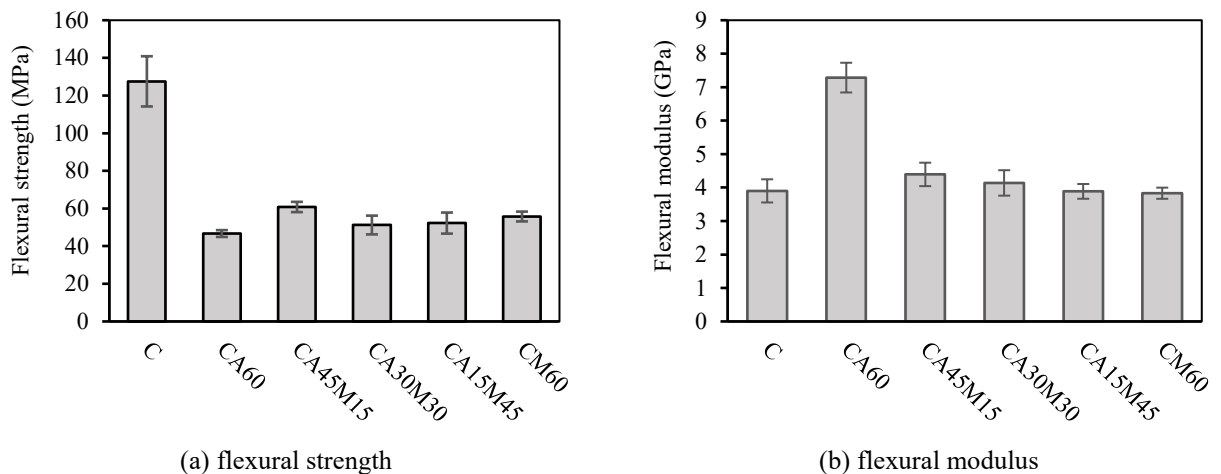
Figure 2(a) shows the flexural strength of GFRP with the addition of ATH only. The graph shows that the increase of ATH content decreases the flexural strength of GFRP, ranging from 34.3% to 63.4% lower than sample C. This is because ATH is a mineral that tends to agglomerate when mixed with resin, which could be attributed to mechanical properties degradation [44]. The agglomeration is resulted from a non-homogeneous particle distribution hence weakening the interaction between the filler and the matrix [42] and leads to a potential stress concentration [46]. The visual observation about such agglomeration will be discussed further in the next section below. On the other hand, Figure 2(b) shows the flexural modulus of GFRP filled with ATH only. It can be seen that the increase of ATH content, which is known as a rigid particle that is hard to deform, increases the flexural modulus of GRFP by up to 86.7% higher than sample C. This

result is in good agreement with the previous results that also show a tendency of reduction in terms of tensile strength, impact strength, and elongation, while the modulus of elasticity is increased [47][48][49].



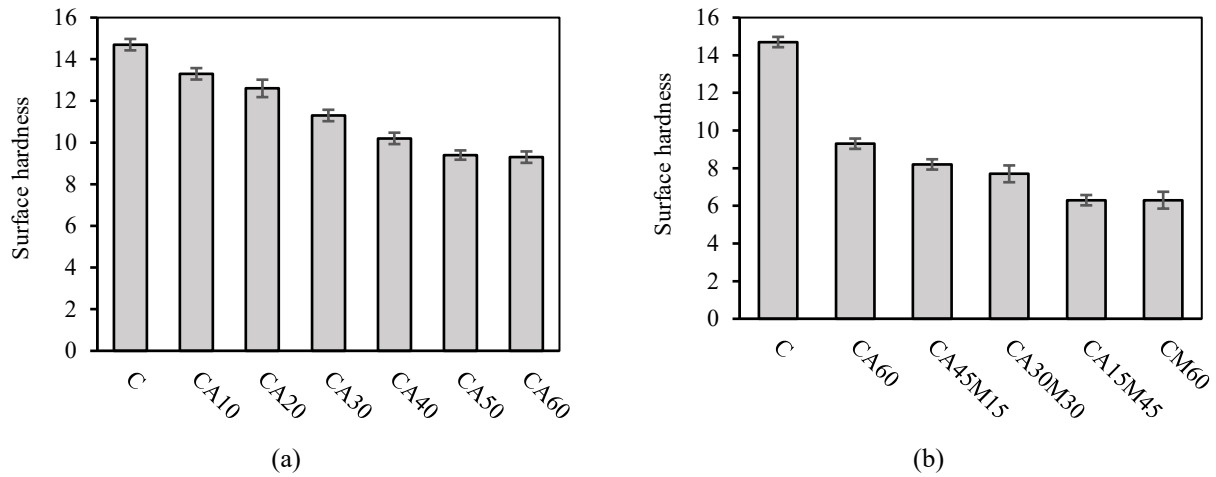
**Figure 2.** Mechanical properties of the GFRP samples filled with ATH.

Figure 3 shows the flexural strength and modulus comparison of GFRP filled with ATH and MMT, neat GFRP (sample C), and a sample of GFRP filled with MMT only (CM60). Figure 3(a) shows a slight increase of flexural strength in the CA45M15 compared to the CA60. Meanwhile, the samples CA30M30 and CA45M15 show relatively the same flexural strength as CA60. Therefore it can be concluded that the addition of MMT mixed with ATH as fillers does not substantially change the flexural strength of GFRP. The pristine MMT is known as a material that is easy to agglomerate and hard to intercalate inside the matrix [50][51]. Furthermore, this result indicates that the ATH and pristine MMT particles fail to make adequate surface interaction [52]. With regards to flexural modulus, it is found that the samples with MMT tend to be less rigid than the GFRP with ATH only (CA60) but almost the same value as the neat GFRP.



**Figure 3.** Mechanical properties of the GFRP samples filled with ATH and MMT.

The bonding quality between the matrix and filler can be indicated by the value of the surface hardness and voids. Figure 4(a) shows the surface hardness of GFRP filled with ATH. The base sample C shows the highest surface hardness of 14.7. The increase of ATH addition leads to a decrease in the surface hardness of the composites by 9.5% to 36.7%. Furthermore, Figure 4(b) shows the surface hardness of GFRP filled with ATH and MMT. The addition of ATH and MMT decreases the surface hardness more significantly, that is, from 44.2% to 57.1%. When comparing the samples with the same amount of filler compositions, that is, the samples CA60 and CM60, the GFRP with MMT filler shows a notably lower surface hardness value than the GFRP with ATH filler. As tabulated in Table 2, the addition of filler particles in the UP resin increases the number of voids and produces easily deformed composites due to a decrease in the hardness [47]. Similar indications were also given of the contribution of voids that might cause a decrease in flexural strength, as in Figure 3(a). In a study of fibre-reinforced polymer composites, an increase in voids can lead to a decrease in flexural strength [53]. The voids are the result of low interfacial bonding between filler and matrix [52]. The lowest percentage of void content was obtained by base sample C at 0.9%, while the highest was found in sample CM60 by 23.9%. It is found that the addition of MMT creates more voids inside the GFRP composites.



**Figure 4.** Surface hardness of GFRP: (a) filled with ATH and (b) filled with ATH and MMT.

**Table 2.** Void contents of the samples used in this study.

Sample name	Void content (%)
C	0.9
CA10	5.9
CA20	12.0
CA30	9.5
CA40	14.2
CA50	14.7
CA60	15.8
CA45M15	18.0
CA30M30	20.5
CA15M45	23.2
CM60	23.9

### Morphology of the Flexural Fractured Surface

The morphological observations of the flexural fractured surface were performed on samples CA60, CA30M30, and CM60 by means of a scanning electron microscope (SEM). The observations were focused on the interaction between the particular filler and the matrix. The morphology of the flexural fractured surface of sample CA60 is shown in Figure 5(a), which shows the tendency of ATH particles to form agglomeration. The holes result from the pulled-out of ATH particles that leave a smooth surface cavity. This smooth surface indicates the weak interfacial bonding between ATH and UP. The high ATH content leads to a non-uniform particle distribution and makes less dispersion to the matrix [47]. The stress concentration in the particles due to high ATH content that causing a lack of dispersing to the matrix, thus resulting in a decrease in the composite mechanical properties [54]. Agglomeration effectively reduces the interfacial area between filler and matrix [21]. Figure 5(b) shows that the sample CA30M30 gives evidence of some agglomerated particles that were pulled out and others split up. Particles with white spots can be either ATH or MMT agglomerations. Furthermore, Figure 5(c) shows that the MMT particle in CM60 also tends to form agglomeration as the ATH. The agglomeration of pristine MMT indicates that the particle cannot disperse well with the matrix, thus resulting in an immiscible system inside the composites [37]. The immiscible pristine MMT particles were formed from the hydrophilic pristine MMT layer wrapped up by hydrophobic material (UP) [18]. However, pristine MMT was successful in improving the mechanical properties of the hydrophilic biopolymer [55]. Agglomeration of the MMT can occur before effective interaction with UP is formed during composites preparation [56]. The holes observed from sample CM60 result from the pulling out of the MMT particles. The pulled-out particle was caused by a weak bond between pristine MMT and the UP [30]. However, there was a notable difference between the sample CA60 and CM60. By visual observation, the sample CA60 has more pulled-out particles than the sample CM60. The CM60 has a split particle which shows a higher flexural strength than the CA60. The split particles left in the matrix indicate an increase in the flexural strength due to the better dispersion in the UP. In good agreement with the previous discussions related to Figure 3, the CA60 shows a lower flexural strength and higher flexural modulus than the CM60.

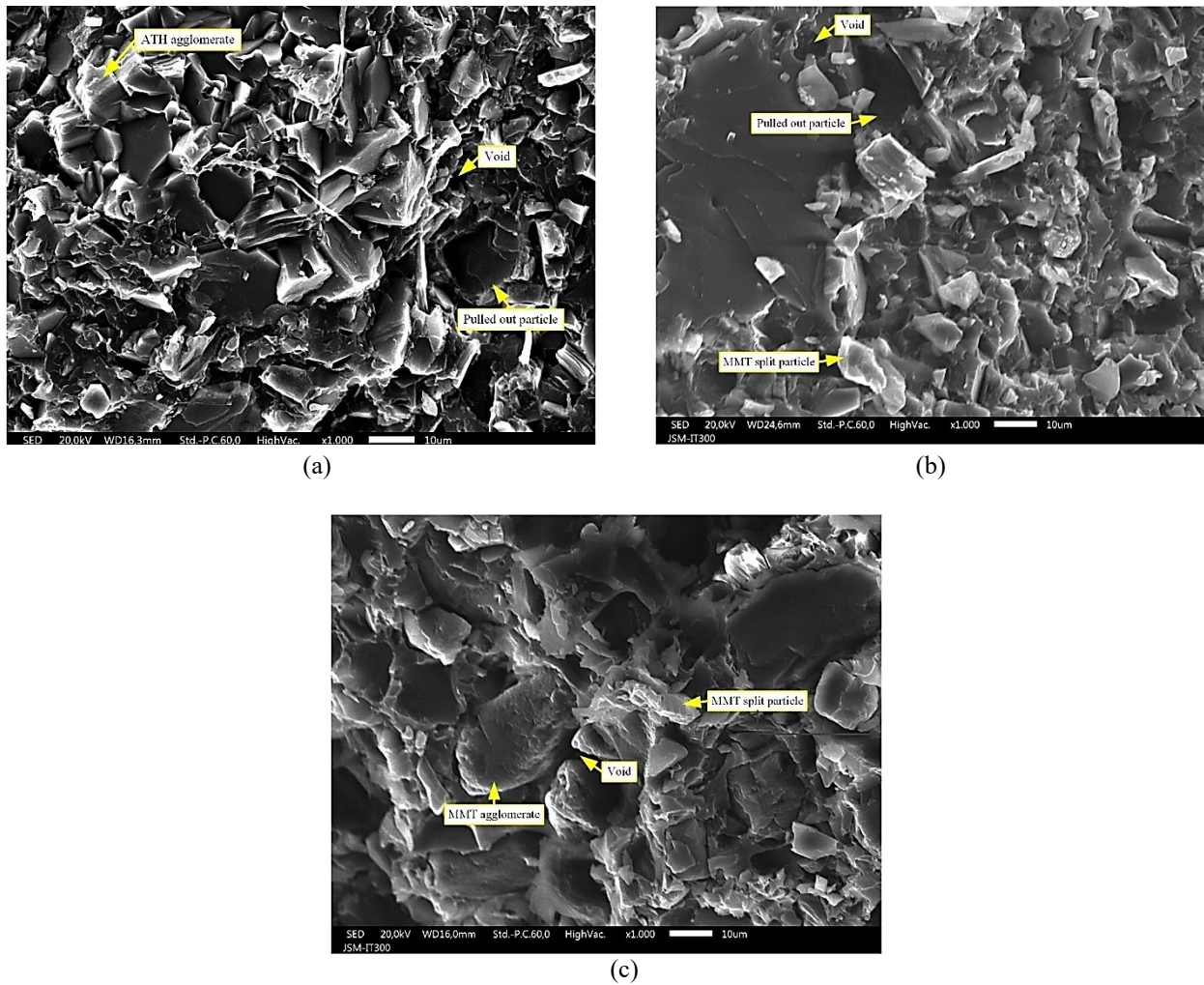


**Figure 5.** Morphology of the flexural fractured surface of (a) CA60, (b) CA30M30, (c) CM60.

### Thermograms Result

The TGA and DTG measurement in Figure 6 were performed for samples C, CA30, CA60, CA30M30, and CM60, especially in the samples matrix and fillers (the GF was excluded in the TGA test). The tested samples show a loss of moisture to a temperature of 250 °C, which is in good agreement with Mourits and Gibson (2006) [37]. At a temperature of 250 °C, as tabulated in Table 3, the sample CA30 has a mass degradation ( $m_{250}$ ) lower than sample C, probably due to the lower UP composition in the GFRP matrix. Meanwhile, the samples CA60, CA30M30, and CM60, which are samples with the same mass percentage of fillers in the UP, show a different  $m_{250}$ . It is found that the addition of MMT increases the  $m_{250}$  of the UP. Based on the previous SEM observation, it is known that the MMT particles tended to form agglomeration in the UP. The agglomeration consisted of a group of hydrophilic MMT which keep the intercalated water inside the layer [18]. At ambient temperatures, MMT works to absorb moisture from the surrounding environment. Furthermore, this material releases water vapour gradually as the temperature increases. The MMT can increase the moisture content in the composite [57]. The increase in the MMT content increases the intercalated water content, which was lost at a temperature of 100-250 °C [58]. The sample of CM60 shows higher mass degradation than CA30M30 because of a higher content of MMT. The TGA result shows that UP filled with ATH yield better thermal stability than UP filled with MMT.

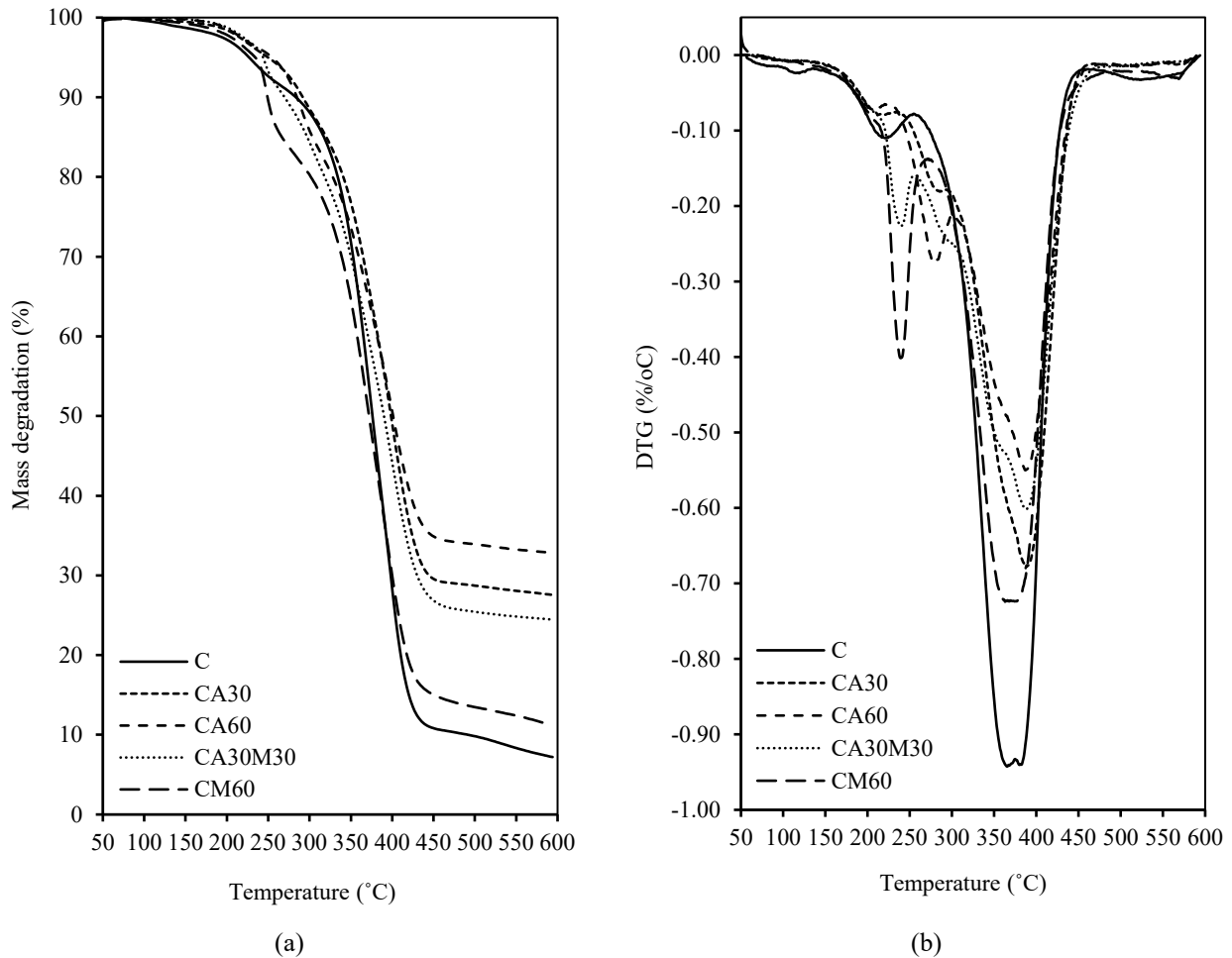


**Figure 6.** Thermograms of (a) TGA and (b) DTG.

The ATH content in the GFRP matrix increases the decomposition temperature at the mass degradation of 50%, indicated by  $T_{50}$  in Table 3. The addition of ATH filler to UP resulted in an increase in  $T_{50}$  to a temperature of about 400 °C. CA30 and CA60 show almost the same values. Conversely, the addition of MMT filler showed a lower  $T_{50}$  than the addition of ATH filler; even CM60 was valued at 5 °C lower than C. These results indicate that MMT carries more moisture content than ATH, which is in good agreement with [57]. Until reaching  $T_{50}$ , samples with MMT were likely to experience higher mass degradation than those without MMT. Regarding the interaction between MMT and UP, another study explains that a high MMT content is not effective in increasing the composites thermal stability due to its low dispersion with the UP [54]. The reduction of decomposition temperature due to the addition of MMT is caused by the clay layer, which absorbs the water, and the activity of the hydroxyl group, which accelerates the decomposition of polyester [58]. The hydroxyl functional group (-OH) of MMT undergoes dehydroxylation with increasing exposure to temperature [59][60]. The  $T_{50}$  of sample CA30M30 is higher than the sample C by 13.0°C. The results of other studies indicate that the combination of ATH and MMT can increase the thermal stability of EVA composites [61].

**Table 3.** TGA and DTG results.

Sample	TGA				DTG			
	$m_{250}$ <sup>1</sup> (%)	$T_{50}$ <sup>2</sup> (°C)	$T_{onset}$ (°C)	Residue (%)	$T_{MMT\_peak}$ (°C)	$T_{ATH\_peak}$ (°C)	$T_{UP\_peak}$ (°C)	$MLR_{max}$ (%/°C)
C	7.4	377.0	337.4	11.4	-	-	390.0	0.95
CA30	4.8	400.0	349.7	29.5	-	285.1	397.2	0.69
CA60	4.9	401.0	351.0	34.8	-	280.1	396.0	0.58
CA30M30	6.8	390.0	349.3	26.4	237.6	-	398.0	0.60
CM60	9.5	372.0	337.5	15.3	238.4	-	388.6	0.72

<sup>1</sup>) Mass degradation at 250 °C

<sup>2</sup>) Temperature when the mass reduced to 50%

The initial temperature of decomposition of the samples is shown as  $T_{onset}$  in Table 3. The addition of ATH leads to a slight increase in  $T_{onset}$ . The 30% of ATH loading does not have a significant effect on UP decomposition [22]. Contrarily, the addition of MMT does not increase the  $T_{onset}$  as indicated by the similar  $T_{onset}$  of samples C and CM60. The CA30M30 shows an increase in  $T_{onset}$  by 11.9°C as compared to sample C.  $T_{onset}$  in all samples showed temperatures between 300 °C

and 400 °C, according to the UP character used in this article [24]. Meanwhile, another study shows that the MMT addition does not influence EVA's initial decomposition temperature ( $T_{\text{onset}}$ ) [62]. The  $T_{\text{onset}}$  of CA30M30 is slightly lower than CA30, even in the same ATH content. The MMT can act as a barrier that can protect the material beneath it from heating, but it can also act as a catalyst for polymer degradation that causes a decrease in thermal stability [63]. The latter is likely due to the catalyst effect of the MMT, which works in contrast to the flame retardancy mechanism of the ATH. Hydroxyl content in MMT [59] may be the cause of the decrease in sample flame retardancy.

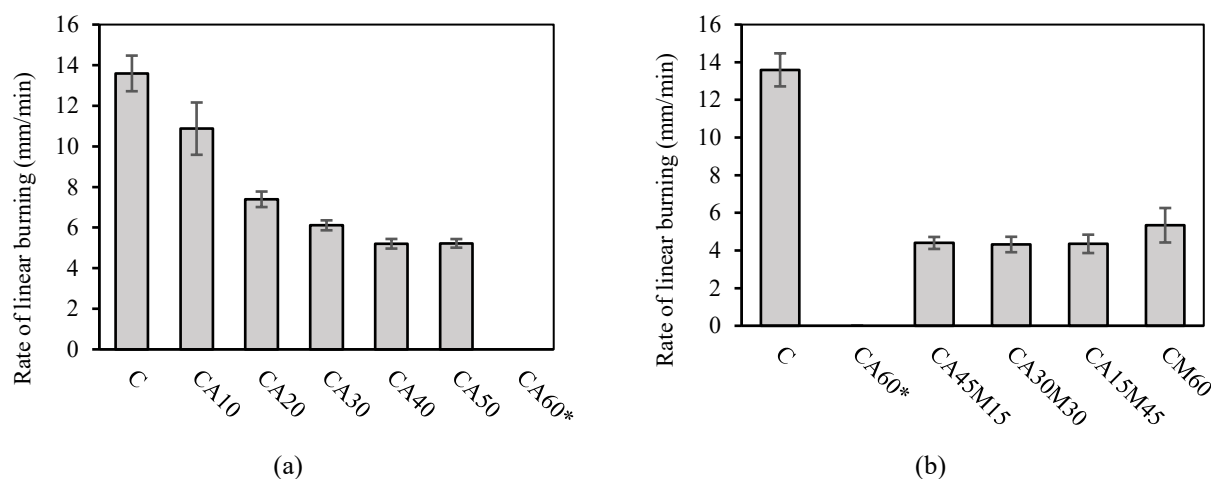
As the temperature became higher than 450°C in Figure 6(a), the flat trends indicate the residue of the samples. The residue in sample C is 11.4% at a temperature of about 500°C, corresponding to the carbon char formation [36]. The residue percentage of CA30 and CA60 increases proportionally to the addition of ATH. The residue in samples CA30 and CA60 is alumina, which has a melting temperature ( $T_m$ ) of 2,054°C, which is much higher than UP [22][24]. Therefore, alumina is an inert material that forms a barrier layer in the decomposition of UP. The increase of residue percentage in a sample of CM60 is due to the MMT addition. The MMT material composition consists of alumina and silica that have higher melting temperatures than the UP. The increase of residue percentage in a sample of CA30M30 is due to the combination of alumina from ATH and silica from MMT. The formation of residue increased even with a slight addition of MMT [64].

Figure 6(b) depicts the DTG thermograms that explain the decomposition rate and stages of the samples. The first stage is the loss of moisture in the matrix low-weight molecule volatiles [37][65][66]. This stage occurs at a temperature below 100°C. All the TGA samples show a small loss of moisture in this stage that is probably caused by post-cured treatment before the test. The second stage is fillers decomposition (ATH and MMT). The MMT decomposition occurs at a temperature of less than 250°C. According to Table 3, the samples of CA30M30 and CM60 show a relatively similar MMT decomposition temperature ( $T_{\text{MMT\_peak}}$ ) of 237.6°C and 238.4°C, respectively. The pristine MMT used in the study is a hydrophilic clay that is easy to absorb water [18]. The MMT decomposition shows the loss of intercalated water to the edge and surface of the clay [44]. The samples of CA30 and CA60 (Table 3) also show relatively similar ATH decomposition temperatures ( $T_{\text{ATH\_peak}}$ ). The decomposition temperature of ATH occurs at a temperature of 220-400 °C with the decomposition products of alumina and water vapour [24][37]. The decomposition temperature of ATH is higher than MMT. The third stage is the decomposition of UP, which starts with the scission of the crosslinks, then followed by the solvent monomer volatilisation and the scission of pre-polymer chains [37]. The addition of ATH and MMT does not show significant changes in the UP decomposition temperature ( $T_{\text{UP\_peak}}$ ). Table 3 also shows that the addition of ATH and MMT tends to decrease the UP maximum mass loss rate ( $\text{MLR}_{\text{max}}$ ). The  $\text{MLR}_{\text{max}}$  decreases proportionally to the increase of the ATH content [24]. The decrease of  $\text{MLR}_{\text{max}}$  shows improvement in terms of the thermal exposure stability of the samples.

### The Rate of Linear Burning (ROB) of the Composites

Figure 7(a) is the rate of linear burning (ROB) of GFRP filled with ATH. The addition of ATH tends to decrease the ROB as a study conducted by Ameer and Habbeb [67]. According to the ASTM D635-03, a self-extinguish condition is declared for the CA60 as the ignited fire never reached the measurement start mark on the sample. The base sample C shows the highest ROB at 13.6 mm/min. The samples CA40 and CA50 show similar ROB at 5.2 mm/min, probably caused by a similar UP decomposition mechanism. The addition of ATH tends to decrease the ROB, as it causes an increase in the endothermic process of UP decomposition heat. The endothermic process decreases the polymer burn temperature due to the absorption of heat [22]. The increase of hydrated fillers effectively reduces the combustion heat [68]. The endothermic process of ATH is a heat-consuming reaction that prevents combustion [69]. Furthermore, the ATH decomposes and produces water vapour and alumina. The high water vapour concentration causes a decrease in the polymer sample combustion [24]. The water vapour from the decomposition of ATH dilutes the flammable gas from the UP decomposition. The high dilution of flammable gas with water vapour causes more oxygen needed to burn [22]. The alumina from the decomposition of ATH forms a barrier layer that prevents the flammable gas from the UP decomposition mix with the oxygen; thus interference continuously combustion [42]. It can be concluded that during the endothermic process, the water vapour (dilutes the flammable gas) and alumina (form the barrier layer) due to the ATH decomposition would lead to the decrease of the UP decomposition rate.

Figure 7(b) depicts a relatively similar ROB for the samples with ATH and MMT, that is, CA45M15, CA30M30, and CA15M45, although the values are also lower than the base sample C. This shows that the combination of ATH and MMT effectively improves the flame retardancy of the GFRP. The MMT increases the flame retardancy of the composites and is probably due to the loss of intercalated water content at a temperature of 100-250°C [65]. The water vapour dilutes the volatiles of UP decomposition, hence decreasing the flammability of the composites. In these ATH-MMT samples, a self-extinguish condition did not happen as in the CA60. This could be due to the residue of alumina and water vapour from the ATH, which prevents the MMT barrier layer formation when the composite decomposition occurs [62]. Another factor that may also occur is the hydroxyl from MMT which is released then reacts with oxygen and becomes reactive [70]. This is contrary to the purpose of MMT as a flame retardant, which is to switch functions to accelerate the decomposition of polyester [58].



\*) CA60 shows a self-extinguish condition before reach the measurement start mark.

**Figure 7.** The rate of linear burning of GFRP: (a) filled with ATH and (b) filled with ATH and MMT.

The decrease of ROB due to the addition of ATH has the same tendencies with the  $MLR_{max}$  from the TGA result (in Table 3). The  $MLR_{max}$  of CA30 and CA60 decreases from 0.69 %/°C to 0.58 %/°C. While the ROB of CA30 and CA60 also decreases from 6.1 mm/min to 0.0 mm/min. It can be concluded that the increase of ATH content results in the decrease of the  $MLR_{max}$  and the ROB. Contrarily, the increase of MMT content in the combination of ATH and MMT increases the  $MLR_{max}$  and the ROB. Furthermore, the addition of ATH is more effective in reducing the  $MLR_{max}$  and the ROB than MMT in the UP-GF composites. The addition of ATH and MMT does not show significant changes in the UP decomposition temperature ( $T_{UP\_peak}$ ).

## CONCLUSION

The combination of ATH and MMT as a flame retardant in the GFRP composites was experimentally evaluated in terms of both the material strength and the flame retardancy. There is a tendency of mechanical properties degradation due to the addition of ATH, MMT, or a combination of both fillers in GFRP. However, the addition of filler ATH, MMT, or a combination of both could increase the flame retardancy of GFRP. The increase of ATH content to UP decreases the flexural strength of GFRP, ranging from 34.3% to 63.4% lower than sample C and increases the flexural modulus of GFRP to approximately 86.7% higher than sample C. A slight increase of flexural strength is found in the CA45M15, but the other two samples, namely CA30M30 and CA45M15, show a relatively same value compared with CA60. This result indicates that the addition of MMT does not dramatically change the flexural strength of GFRP. Regarding the bonding quality between the matrix and the filler, the increase of ATH content reduces the surface hardness of the composites by 9.5% to 36.7% and notably increases the voids than the neat GFRP. The addition of MMT shows much lower surface hardness and more voids than the GFRP with ATH only.

According to the morphology of the flexural fractured sample, the ATH particles tended to form agglomeration and pulled-out of the UP. The smooth surface cavity demonstrates a weak interfacial bonding between ATH and UP. Similarly, MMT particles in the composites also tend to form agglomeration, but with a relatively better interfacial bonding. The addition of ATH leads to a small increase in the initial temperature of decomposition (Tonset). In contrast, the addition of MMT does not increase the Tonset, as indicated by a similar value with sample C. The DTG result shows that the decomposition temperature of ATH is higher than MMT, although the addition of ATH and MMT does not show significant changes in the UP decomposition temperature. However, the addition of ATH and MMT tends to decrease the UP maximum mass loss rate. The flammability test of the samples shows that the addition of ATH tends to reduce the rate of linear burning (ROB) from 20.0% to 100.0% (self-extinguish) than the neat GFRP. The CA60 is the only sample that the ignited fire never reach the measurement start mark in the test. The combination of ATH and MMT also effectively improves the flame retardancy of the GFRP. Furthermore, MMT in GFRP increases the flame retardancy of GFRP even though it did not reach self-extinguish condition. This study demonstrates that the composition and combination of ATH and MMT fillers accordingly could produce optimal mechanical properties and flame retardancy.

## ACKNOWLEDGEMENT

The authors acknowledge the facilities, scientific and technical support from Bandung Advanced Characterization Laboratories in National Research and Innovation Agency. S. Kaleg is the main contributor of this paper. K. Diharjo and D. Ariawan contributed to the supervision of the research activity. All authors read and approved the final paper.

## REFERENCES

- [1] M. Chieruzzi, A. Miliozzi, and J. M. Kenny, "Effects of the nanoparticles on the thermal expansion and mechanical properties of unsaturated polyester/clay nanocomposites," *Compos. Part A Appl. Sci. Manuf.*, vol. 45, pp. 44–48, 2013, doi:

- 10.1016/j.compositesa.2012.09.016.
- [2] J. Maxwell, *Plastics In The Automotive Industry*. Cambridge: Woodhead Publishing, 1994.
  - [3] S. Sudirja, A. Hapid, Amin, S. Kaleg, and A. C. Budiman, "Stress analysis simulations of welded and bolted joints method for full steel and composite-steel chassis structure of electric low floor medium bus," *EUREKA Phys. Eng.*, vol. 6, pp. 72–81, 2020, doi: 10.21303/2461-4262.2020.001516.
  - [4] D. Mann, *Automotive Plastics & Composites*, Second edi. Elsevier, 1999.
  - [5] B. Ravishankar, S. K. Nayak, and M. A. Kader, "Hybrid composites for automotive applications – A review," *J. Reinf. Plast. Compos.*, vol. 38, no. 18, pp. 835–845, 2019, doi: 10.1177/0731684419849708.
  - [6] D. Carlstedt and L. E. Asp, "Performance analysis framework for structural battery composites in electric vehicles," *Compos. Part B Eng.*, vol. 186, no. January, p. 107822, 2020, doi: 10.1016/j.compositesb.2020.107822.
  - [7] A. R. Horrocks and D. Price, *Advances in Fire Retardant Materials*, Cambridge: Woodhead Publishing, 2008.
  - [8] N. Grange et al., "Fire resistance of carbon-based composite materials under both ideal and realistic normative configurations," *Appl. Therm. Eng.*, vol. 159, no. November 2018, p. 113834, 2019, doi: 10.1016/j.applthermaleng.2019.113834.
  - [9] A. B. Morgan, G. Knapp, S. I. Stoliarov, and S. V. Levchik, "Studying smoldering to flaming transition in polyurethane furniture subassemblies: Effects of fabrics, flame retardants, and material type," *Fire Mater.*, vol. 45, no. 1, pp. 56–67, 2021, doi: 10.1002/fam.2847.
  - [10] C. Perez-Salinas, C. Castro, G. Patin, F. Peña, and D. Paredes, "Application of flame retardants aluminum hydroxide and magnesium hydroxide in a material composed of glass fibre with polymeric matrix and its influence on the flammability index," *Key Eng. Mater.*, vol. 818 KEM, pp. 128–133, 2019, doi: 10.4028/www.scientific.net/KEM.818.128.
  - [11] A. Patil, A. Patel, and R. Purohit, "An overview of Polymeric Materials for Automotive Applications," *Mater. Today Proc.*, vol. 4, no. 2, pp. 3807–3815, 2017, doi: 10.1016/j.matpr.2017.02.278.
  - [12] N. Sakib and A. K. M. A. Iqbal, "Epoxy based nanocomposite material for automotive application- a short review," *Int. J. Automot. Mech. Eng.*, vol. 18, no. 3, pp. 9127–9140, 2021, doi: DOI: <https://doi.org/10.15282/ijame.18.3.2021.24.0701>.
  - [13] A. Saleem, L. Medina, and M. Skrifvars, "Improvement of performance profile of acrylic based polyester bio-composites by bast/basalt fibres hybridisation for automotive applications," *J. Compos. Sci.*, vol. 5, no. 4, 2021, doi: 10.3390/jcs5040100.
  - [14] P. E. Romero, J. Arribas-Barrios, O. Rodriguez-Alabanda, R. González-Merino, and G. Guerrero-Vaca, "Manufacture of polyurethane foam parts for automotive industry using FDM 3D printed molds," *CIRP J. Manuf. Sci. Technol.*, vol. 32, pp. 396–404, 2021, doi: 10.1016/j.cirpj.2021.01.019.
  - [15] J. Gupta, N. Reynolds, T. Chiciudean, and K. Kendall, "A comparative study between epoxy and vinyl ester CF-SMC for high volume automotive composite crash structures," *Compos. Struct.*, vol. 244, no. March, p. 112299, 2020, doi: 10.1016/j.compstruct.2020.112299.
  - [16] T. Pepper, "Polyester Resins," in *ASM Handbook: Composites*, vol. 21, ASM International, 2001.
  - [17] C. M. C. Pereira, M. Herrero, F. M. Labajos, A. T. Marques, and V. Rives, "Preparation and properties of new flame retardant unsaturated polyester nanocomposites based on layered double hydroxides," *Polym. Degrad. Stab.*, vol. 94, no. 6, pp. 939–946, 2009, doi: 10.1016/j.polymdegradstab.2009.03.009.
  - [18] S. Levchik, "Phosphorus-based FRs," in *Non-Halogenated Flame Retardant Handbook*, A. B. Morgan and C. A. Wilkie, Eds. John Wiley & Sons, Ltd., 2014, pp. 43–45.
  - [19] J. Zhou, M. Xu, X. Zhang, Y. Leng, Y. He, and B. Li, "Preparation of highly efficient flame retardant unsaturated polyester resin by exerting the fire resistant effect in gaseous and condensed phase simultaneously," *Polym. Adv. Technol.*, vol. 30, no. 7, pp. 1684–1695, 2019, doi: 10.1002/pat.4599.
  - [20] F. Chu et al., "Hierarchical core-shell TiO<sub>2</sub>@LDH@Ni(OH)<sub>2</sub> architecture with regularly-oriented nanocatalyst shells: Towards improving the mechanical performance, flame retardancy and toxic smoke suppression of unsaturated polyester resin," *Chem. Eng. J.*, vol. 405, no. August 2020, p. 126650, 2021, doi: 10.1016/j.cej.2020.126650.
  - [21] M. Zhang, W. Ye, and Z. Liao, "Preparation, characterisation and properties of flame retardant unsaturated polyester resin based on r-PET," *J. Polym. Environ.*, no. 0123456789, 2021, doi: 10.1007/s10924-021-02325-w.
  - [22] N. Maheshwari, S. Thakur, P. Neogi, and S. Neogi, "UV resistance and fire retardant property enhancement of unsaturated polyester composite," *Springer Polym. Bull.*, 2015, doi: 10.1007/s00289-015-1346-z.
  - [23] G. Chai, G. Zhu, S. Gao, J. Zhou, Y. Gao, and Y. Wang, "On improving flame retardant and smoke suppression efficiency of epoxy resin doped with aluminum tri-hydroxide," *Adv. Compos. Lett.*, vol. 28, pp. 1–12, 2019, doi: 10.1177/2633366X19894597.
  - [24] T. D. Hapuarachchi and T. Peijs, "Aluminium trihydroxide in combination with ammonium polyphosphate as flame retardants for unsaturated," *Express Polym. Lett.*, vol. 3, no. 11, pp. 743–751, 2009, doi: 10.3144/expresspolymlett.2009.92.
  - [25] A. Perthue, P. Bussiere, M. Baba, J. Larche, J. Gardette, and S. Therias, "Correlation between water uptake and loss of the insulating properties of PE / ATH composites used in cables applications," *Polym. Degrad. Stab. J.*, vol. 127, 2016, doi: 10.1016/j.polymdegradstab.2016.01.020.
  - [26] S. Han, X. Zhu, F. Chen, S. Chen, and H. Liu, "Flame-retardant system for rigid polyurethane foams based on diethyl bis(2-hydroxyethyl)aminomethylphosphonate and in-situ exfoliated clay," *Polym. Degrad. Stab.*, vol. 177, p. 109178, 2020, doi: 10.1016/j.polymdegradstab.2020.109178.
  - [27] M. Jiang et al., "Flame retardancy of unsaturated polyester composites with modified ammonium polyphosphate, montmorillonite, and zinc borate," *J. Appl. Polym. Sci.*, vol. 136, no. 11, pp. 20–22, 2019, doi: 10.1002/app.47180.
  - [28] X. Wang et al., "Halogen-free intumescent flame-retardant ethylene-vinyl acetate copolymer system based on organic montmorillonite and graphene nanosheets," *J. Appl. Polym. Sci.*, vol. 135, no. 23, pp. 1–10, 2018, doi: 10.1002/app.46361.
  - [29] P. M. Visakh and Y. Arao, *Flame Retardants Polymer Blends, Composites and Nanocomposites*. Springer, 2015.
  - [30] D. Romanzini, A. Frache, A. J. Zattera, and S. C. Amico, "Effect of clay silylation on curing and mechanical and thermal properties of unsaturated polyester/montmorillonite nanocomposites," *J. Phys. Chem. Solids*, vol. 87, pp. 9–15, 2015, doi: 10.1016/j.jpcs.2015.07.019.
  - [31] K. Diharjo, V. B. Armunanto, and S. A. Kristiawan, "Tensile and burning properties of clay / phenolic / GF composite and its application," *AIP Conf. Proc.*, vol. 040024, 2016, doi: 10.1063/1.4943467.
  - [32] M. Indra Reddy, M. Anil Kumar, and C. Rama Bhadri Raju, "Tensile and flexural properties of jute, pineapple leaf and glass fibre reinforced polymer matrix hybrid composites," in *Materials Today: Proceedings*, 2018, vol. 5, no. 1, pp. 458–462, doi:

- 10.1016/j.matpr.2017.11.105.
- [33] C. Annandarajah, A. Langhorst, A. Kiziltas, D. Grewell, D. Mielewski, and R. Montazami, "Hybrid cellulose-glass fibre composites for automotive applications," *Materials (Basel)*, vol. 12, no. 19, pp. 1–11, 2019, doi: 10.3390/ma12193189.
- [34] M. R. Petersen, A. Chen, M. Roll, S. J. Jung, and M. Yossef, "Mechanical properties of fire-retardant glass fibre-reinforced polymer materials with alumina tri-hydrate filler," *Compos. Part B*, vol. 78, pp. 109–121, 2015, doi: 10.1016/j.compositesb.2015.03.071.
- [35] S. Kaleg, D. Ariawan, and K. Diharjo, "The flexural strength of glass fibre reinforced polyester filled with aluminum tri-hydroxide and montmorillonite," in *Key Engineering Materials*, 2018, vol. 772, pp. 28–32, doi: 10.4028/www.scientific.net/KEM.772.28.
- [36] L. Tibiletti *et al.*, "Thermal degradation and fire behaviour of unsaturated polyesters filled with metallic oxides," *Polym. Degrad. Stab.*, vol. 96, no. 1, pp. 67–75, 2011, doi: 10.1016/j.polymdegradstab.2010.10.015.
- [37] A. P. Mouritz and A. G. Gibson, *Fire Properties of Polymer Composite Materials*. Springer, 2006.
- [38] Riyazuddin, T. N. Rao, I. Hussain, and B. H. Koo, "Effect of aluminum tri-hydroxide/zinc borate and aluminium tri-hydroxide/melamine flame retardant systems synergies on epoxy resin," in *Materials Today: Proceedings*, 2019, vol. 27, no. 3, pp. 2269–2272, doi: 10.1016/j.matpr.2019.09.110.
- [39] F. Uddin, "Montmorillonite: An Introduction to Properties and Utilisation," in *Current Topics in the Utilisation of Clay in Industrial and Medical Applications*, 2018, pp. 3–24.
- [40] X. Li *et al.*, "Synergistic effect of amino silane functional montmorillonite on intumescent flame-retarded SEBS and its mechanism," *J. Appl. Polym. Sci.*, vol. 134, no. 24, pp. 1–11, 2017, doi: 10.1002/app.44953.
- [41] F. T. Wallenberger, J. C. Watson, and H. Li, "Glass Fibres," in *ASM Handbook: Composites*, vol. 21, ASM International, 2001.
- [42] R. Baskaran, M. Sarojadevi, and C. T. Vijayakumar, "Unsaturated polyester nanocomposites filled with nano alumina," *Springer J Mater Sci*, no. December 2010, pp. 4864–4871, 2011, doi: 10.1007/s10853-011-5398-7.
- [43] K. Laoubi, Z. Hamadi, A. Ahmed Benyahia, A. Serier, and Z. Azari, "Thermal behavior of E-glass fibre-reinforced unsaturated polyester composites," *Compos. Part B Eng.*, vol. 56, pp. 520–526, 2014, doi: 10.1016/j.compositesb.2013.08.085.
- [44] D. Romanzini, V. Piroli, A. Frache, A. J. Zattera, and S. C. Amico, "Sodium montmorillonite modified with methacryloxy and vinylsilanes : Influence of silylation on the morphology of clay / unsaturated polyester nanocomposites," *Appl. Clay Sci.*, vol. 114, pp. 550–557, 2015, doi: 10.1016/j.clay.2015.07.003.
- [45] C. Campana, R. Leger, R. Sonnier, L. Ferry, and P. Ienny, "Effect of post curing temperature on mechanical properties of a flax fibre reinforced epoxy composite," *Compos. Part A Appl. Sci. Manuf.*, vol. 107, pp. 171–179, 2018, doi: 10.1016/j.compositesa.2017.12.029.
- [46] T. O. Suoware, S. O. Edelugo, B. N. Ugwu, E. Amula, and I. E. Digitemie, "Development of flame retarded composite fibreboard for building applications using oil palm residue," *Mater. Constr.*, vol. 69, no. 335, pp. 1–8, 2019, doi: 10.3989/mc.2019.10418.
- [47] S. Y. Fu, X. Q. Feng, B. Lauke, and Y. W. Mai, "Effects of particle size, particle/matrix interface adhesion and particle loading on mechanical properties of particulate-polymer composites," *Compos. Part B Eng.*, vol. 39, no. 6, pp. 933–961, 2008, doi: 10.1016/j.compositesb.2008.01.002.
- [48] Q. Zhao, Z. Jia, X. Li, and Z. Ye, "Effect of Al (OH)<sub>3</sub> particle fraction on mechanical properties of particle-reinforced composites using unsaturated polyester as matrix," *Fail. Anal. Preven.*, pp. 515–519, 2010, doi: 10.1007/s11668-010-9379-y.
- [49] C. F. Pérez-Salinas, C. B. Castro, E. R. Valencia, and O. F. Freire, "Influence of flame retardants on the mechanical properties of glass fibre reinforced composites in polymeric matrix epoxy and polyester," in *IOP Conference Series: Materials Science and Engineering*, 2019, vol. 628, no. 1, doi: 10.1088/1757-899X/628/1/012001.
- [50] A. B. Inceoglu and U. Yilmazer, "Mechanical properties of unsaturated polyester / montmorillonite composites," *MRS Proc.*, vol. 703, 2001, doi: 10.1557/PROC-703-V9.23.
- [51] C. Shuai, B. Peng, M. Liu, S. Peng, and P. Feng, "A self-assembled montmorillonite-carbon nanotube hybrid nanoreinforcement for poly-L-lactic acid bone scaffold," *Mater. Today Adv.*, vol. 11, p. 100158, 2021, doi: 10.1016/j.mtaadv.2021.100158.
- [52] K. Diharjo, N. S. Suharty, A. E. B. Nusantara, and R. Afandi, "The effect of sokka clay on the tensile and burning properties of rPP/clay composite," *Adv. Mater. Res.*, vol. 1123, pp. 338–342, 2015, doi: 10.4028/www.scientific.net/AMR.1123.338.
- [53] D. K. Rajak, D. D. Pagar, P. L. Menezes, and E. Linul, "Fibre-reinforced polymer composites: Manufacturing, properties, and applications," *Polymers (Basel)*, vol. 11, no. 10, 2019, doi: 10.3390/polym11101667.
- [54] M. A. Vargas, H. Vázquez, and G. Guthausen, "Non-isothermal curing kinetics and physical properties of MMT-reinforced unsaturated polyester (UP) resins," *Thermochim. Acta*, vol. 611, pp. 10–19, 2015, doi: 10.1016/j.tca.2014.12.024.
- [55] I. Derungs, M. Rico, J. López, L. Barral, B. Montero, and R. Bouza, "Influence of the hydrophilicity of montmorillonite on structure and properties of thermoplastic wheat starch/montmorillonite bionanocomposites," *Polym. Adv. Technol.*, vol. 32, no. 11, pp. 4479–4489, 2021, doi: 10.1002/pat.5450.
- [56] Y. Zahedi, B. Fathi-Achachlouei, and A. R. Yousefi, "Physical and mechanical properties of hybrid montmorillonite/zinc oxide reinforced carboxymethyl cellulose nanocomposites," *Int. J. Biol. Macromol.*, vol. 108, pp. 863–873, 2018, doi: 10.1016/j.ijbiomac.2017.10.185.
- [57] B. Fathi Achachlouei and Y. Zahedi, "Fabrication and characterisation of CMC-based nanocomposites reinforced with sodium montmorillonite and TiO<sub>2</sub> nanomaterials," *Carbohydr. Polym.*, vol. 199, no. July, pp. 415–425, 2018, doi: 10.1016/j.carbpol.2018.07.031.
- [58] W. Yang, Y. Hu, Q. Tai, H. Lu, L. Song, and R. K. K. Yuen, "Fire and mechanical performance of nanoclay reinforced glass-fibre/PBT composites containing aluminum hypophosphite particles," *Compos. Part A*, vol. 42, no. 7, pp. 794–800, 2011, doi: 10.1016/j.compositesa.2011.03.009.
- [59] K. Vaezi, G. Asadpour, and H. Sharifi, "Effect of ZnO nanoparticles on the mechanical, barrier and optical properties of thermoplastic cationic starch/montmorillonite biodegradable films," *Int. J. Biol. Macromol.*, vol. 124, pp. 519–529, 2019, doi: 10.1016/j.ijbiomac.2018.11.142.
- [60] Y. Qin, T. Peng, H. Sun, L. Zeng, Y. Li, and C. Zhou, "Effect of montmorillonite layer charge on the thermal stability of bentonite," *Clays Clay Miner.*, vol. 69, no. 3, pp. 328–338, 2021, doi: 10.1007/s42860-021-00117-w.
- [61] Y. Yen, H. Wang, and W. Guo, "Synergistic flame retardant effect of metal hydroxide and nanoclay in EVA composites," *Polym. Degrad. Stab.*, vol. 97, no. 6, pp. 863–869, 2012, doi: 10.1016/j.polymdegradstab.2012.03.043.

- [62] M. Chang, S. Hwang, and S. Liu, "Flame retardancy and thermal stability of ethylene-vinyl acetate copolymer nanocomposites with alumina trihydrate and montmorillonite," *J. Ind. Eng. Chem.*, vol. 20, no. 4, pp. 1596–1601, 2014, doi: 10.1016/j.jiec.2013.08.004.
- [63] V. P.M. and A. Yoshihiko, *Flame Retardants: Polymer Blends, Composites and Nanocomposites*. Springer, 2015.
- [64] L. Li, X. Mao, R. Ju, Y. Chen, and L. Qian, "Synergistic effect of organo-montmorillonite on intumescent flame-retardant PLA," *Ferroelectrics*, vol. 527, no. 1, pp. 25–36, 2018, doi: 10.1080/00150193.2018.1450045.
- [65] F. Dellisanti, A. Calafato, G. A. Pini, D. Moro, G. Ulian, and G. Valdrè, "Effects of dehydration and grinding on the mechanical shear behaviour of Ca-rich montmorillonite," *Appl. Clay Sci.*, vol. 152, no. August 2017, pp. 239–248, 2018, doi: 10.1016/j.clay.2017.11.019.
- [66] A. Hassan, L. Y. Hau, and M. Hasan, "Effect of ammonium polyphosphate on flame retardancy, thermal stability, and mechanical properties of unsaturated polyester/phenolic/montmorillonite nanocomposites," *Adv. Polym. Technol.*, vol. 36, no. 3, pp. 278–283, 2017, doi: 10.1002/adv.21605.
- [67] Z. J. A. Ameer and D. H. Habbeb, "Effect of polyvinyl alcohol on burning rate for Flexible PVC with addition of magnesium hydroxide and Aluminum tri-hydroxide," *J. Babylon Univ. Sci.*, vol. 25, no. 2, pp. 593–603, 2017.
- [68] R. Sonnier *et al.*, "Fire retardant benefits of combining aluminum hydroxide and silica in ethylene-vinyl acetate copolymer (EVA)," *Polym. Degrad. Stab.*, vol. 128, pp. 228–236, 2016, doi: 10.1016/j.polymdegradstab.2016.03.030.
- [69] N. S. Suharty, K. Dihadjo, and D. S. Handayani, "Effect of single flame retardant aluminum tri-hydroxide and boric acid against inflammability and biodegradability of recycled PP / KF composites," *AIP Conf. Proc.*, vol. 040026, pp. 1–7, 2016, doi: 10.1063/1.4943469.
- [70] Y. Wang *et al.*, "Suppression effects of hydroxy acid modified montmorillonite powders on methane explosions," *Energies*, vol. 12, no. 21, pp. 1–12, 2019, doi: 10.3390/en12214068.